A quasistatic model for an elastic, plastic, viscous foam

Philippe Marmottant, François Graner

A quasistatic model for an elastic, plastic, viscous foam

Philippe Marmottant and François Graner
Laboratoire de Spectrométrie Physique, CNRS-Université Grenoble I,
B.P. 87, F-38402 St Martin d'Hères Cedex, France.
(Dated: October 9, 2006)

We suggest a scalar model for deformation and flow a of an amorphous material such as a foam or an emulsion. To describe elastic, plastic and viscous behaviours, we use three scalar variables: elastic strain, plastic deformation rate and total deformation rate; and three material specific parameters: shear modulus, yield strain and viscosity. We discuss the role of the elastic strain and of the yield function, as well as their link with the microscopical structure. The equations we obtain are quasistatic, that is, limited to deformations and flows slower than the relaxation rate towards mechanical equilibrium. But they are valid both in transient or steady flow regimes, even at large elastic strain; and we discuss why viscosity can be relevent even in this limit. Predictions of the storage and loss moduli agree well with the experimental literature, and explain with simple arguments the non-linear large amplitude trends.

I. INTRODUCTION

Elastic materials deform reversibly [1]; plastic materials can be sculpted, that is, they can be deformed into a new shape and keep it [2]; and viscous materials flow [3]. A wide variety of materials display a combination of these properties [4–6], such as elasto-plastic metals and rocks, visco-elastic polymer solutions or visco-plastic mineral suspensions.

Foams are visco-elasto-plastic [7–9]: they are elastic at low strain, plastic at high strain and flow under high shear rate. This is also the case for other concentrated suspensions of deformable objects in a liquid [4, 10, 11], such as droplets in emulsions, vesicles suspensions, or red blood cells in blood. Despite a large literature on experiments and simulations [9], we lack an unified theoretical description of foams.

Here we group three key ingredients for a quasistatic model. Elastic strain is a state variable [12] reversibly stored by the foam's microstructure, that is, the shape of bubbles [13, 14]). Yielding is determined by the value of the strain (or equivalently the elastic part of the stress) rather than by the total stress [15, 16]; Microscopic rearrangements are followed by relaxations towards local mechanical equilibrium, which results in energy dissipation analogous to solid friction. Large scale velocity gradients are associated with a fluid-like friction. Each of the three mechanical behaviours is associated with a material specific parameter: elastic modulus, yield strain (or rather yield function) and viscosity.

For simplicity, we assume here that these parameters are constant and the equations are linear. We consider here homogeneous deformation of a material, not depending on space coordinates. We consider only the magnitude of deformation, but not spatial orientation: the material state variables are all scalars. This represents an incompressible material, where the deformation is a pure shear. Although this model is minimal, it is written with enough generality to enable for extensions to higher dimensions using tensors, to higher shear rates, and to other ingredients such as external forces (to be published).

This article is organised as follows. Section II introduces a quasistatic visco-elasto-plastic model (3,eqs. 10) based on two scalar variables: the elastic strain and the shear rate. Section III presents scalar predictions of the storage and loss moduli. They agree with experimental data in a large range of amplitude and deformation rate. The agreement becomes remarkable if we describe the plastic yielding as a gradual transition (eq. 5). Section IV presents three pedagogical representations, including the foam's phase diagram (Fig. 6).

II. MODEL

A. Quasi-static limit

A material is in a quasistatic regime if all control parameters and external perturbations are slower than the material's microscopic relaxation time towards equilibrium $\tau_{\rm relax}$ (or the slowest of all relaxation times, if there are more than one). The material thus evolves (it is not static) but passes through a succession of mechanical equilibrium states.

In foams, bubbles can swap neighbours (topological rearrangements, called "T1 processes" [17–19]). A T1 does not dissipate energy by itself, but it brings the foam in an out-of-equilibrium state; it is thus followed by a dissipation of energy during the relaxation towards another equilibrium configuration. A foam is in quasistatic regime if the rate of T1s, such as caused by coarsening or shearing, is slower than the microscopical relaxation time $\tau_{\rm relax}$ after T1s.

In a quasistatic rheology experiment, the foam spends most of the time at or very close to mechanical equilibrium. Thus Plateau rules [8] are (almost) always satisfied: corrections are of order $\dot{\varepsilon}\tau_{\rm relax}$, with $\dot{\varepsilon}$ the shear rate, and thus negligible here. The elastic deformation is almost independent on the shear rate $\dot{\varepsilon}$, and all velocities scale almost proportionnally to $\dot{\varepsilon}$.

In a rheology experiment, the quasistatic limit - for

the elastic deformation - is thus reached if and only if $\dot{\varepsilon}\tau_{\text{relax}} \ll 1$. This criterion thus regards time scales, and is not a criterion based on the absence or presence of dissipation. In fact, dissipation is absolutely necessary to observe a quasistatic regime: it damps oscillations and decreases the energy when relaxing towards equilibrium.

Viscous dissipative effects can be observed while remaining in the quasistatic regime for the elastic deformation. The viscous effects are mostly visible when considering measurements of the loss modulus at very low amplitude oscillations, and hence at very low shear rate (as presented below in Figs. 3-5). We suspect that most published experiments on foams are actually quasistatic and almost obey Plateau rules, with the notable exceptions of flows at high velocities or in micro-channels.

B. Plasticity

In the elastic regime, the elastic strain U is equal to the total applied deformation on the material, that is, the time integral $\varepsilon = \int \dot{\varepsilon}\ \mathrm{d}t$ of the shear rate. Thus, in an elastic regime, no intrinsic definition of U is necessary.

However, in a plastic regime, the total applied deformation is shared between elastic deformation U and a plastic deformation, the loading rate being:

$$\dot{\varepsilon} = \frac{\mathrm{d}U}{\mathrm{d}t} + \dot{\varepsilon}_P, \tag{1}$$

where $\dot{\varepsilon}_P$ is the plastic deformation rate; its microscopic origin is the rate of topological rearrangements [20]. Thus U and $\dot{\varepsilon}$ become independent variables: for instance in a steady flow, $\mathrm{d}U/\mathrm{d}t = 0$, then $\dot{\varepsilon} = \dot{\varepsilon}_P$ and $\varepsilon = \int \dot{\varepsilon} dt$ does not define the elastic strain. Elastic deformation U requires an independent, intrinsic definition [12, 13], which is possible at least in foams [14, 20]). The problem now is to express how $\dot{\varepsilon}$ is shared between $\mathrm{d}U/\mathrm{d}t$ and $\dot{\varepsilon}_P$.

We must write a relation between these variables, for instance by expressing how $\dot{\varepsilon}_P$ depends of elastic state and of the applied deformation rate: $\dot{\varepsilon}_P(U, \dot{\varepsilon})$. Dimensionnally, both $\dot{\varepsilon}_P$ and $\dot{\varepsilon}$ are in s^{-1}, while U is dimensionless. Thus $\dot{\varepsilon}_P$ scales like $\dot{\varepsilon}$ [20]:

$$\dot{\varepsilon}_P = \mathcal{H}(|U| - U_Y)\ \mathcal{H}(U\dot{\varepsilon})\ \dot{\varepsilon}. \tag{2}$$

We now discuss one by one the different factors in eq. (2).

The first factor is a Heaviside function, which is zero for negative numbers, and 1 for positive numbers, here when the absolute value of deformation $|U|$ exceeds the yield strain U_Y. This describes an abrupt transition from elastic to plastic regime, as could be the case for an ordered foam [21]. This hypothesis will be relaxed in the next section, introducing a more progressive transition.

The second factor characterises the hysteresis. Plastic rearrangements occur only when the deformation rate $\dot{\varepsilon}$ and the current deformation U have the same sign. Else, the deformation rate results in elastic unloading, and the deformation gets smaller than the yield strain.

The third factor indicates that, in a quasistatic motion (where τ_{relax} can play no explicit role), the only relevent time scale to fix the rate of plastic rearrangements is $\dot{\varepsilon}$.

Eq. (2) can be injected in eq. (1):

$$\frac{\mathrm{d}U}{\mathrm{d}t} = \dot{\varepsilon}\ \left[1 - \mathcal{H}(|U| - U_Y)\ \mathcal{H}(U\dot{\varepsilon})\right], \tag{3}$$

which provides an evolution equation of U as a function of the applied shear rate $\dot{\varepsilon}$. Here U_Y appears as the stable value for U, that is, a fixed point;

C. Yield function

1. Definition

In a disordered foam, for instance with a wide distribution of bubble sizes, topological rearrangements do not necessarily occur for the same value of deformation. Thus U_Y is a macroscopic yield strain, where most rearrangements occur. Conversely, the first isolated topological rearrangements might appear at a lower critical value, U_m, characteristic of the microstructure (which can even be close to zero for a very disordered foam).

Such a smooth transition from elasticity to plasticity requires to generalise the postulate (2) as:

$$\dot{\varepsilon}_P = h(U)\,\mathcal{H}(U\dot{\varepsilon})\,\dot{\varepsilon}, \tag{4}$$

that is, using eq. (1):

$$\frac{\mathrm{d}U}{\mathrm{d}t} = \dot{\varepsilon}\ \left[1 - h(U)\,\mathcal{H}(U\dot{\varepsilon})\right], \tag{5}$$

where we introduce the *yield function* $h(U)$. By definition, $h = 0$ corresponds to a purely elastic state where the elastic deformation follows the applied deformation. Conversely, for $h = 1$ the plasticity rate is equal to the deformation rate.

The yield function h depends on the material under consideration, and can in principle be measured experimentally. It should be a growing (or at least non-decreasing) function of U for $U > 0$, and $h(-U) = h(U)$. Moreover, $h(0) = 0$, so that $h(U) \geq 0$ for all U.

Beside that, there is no special requirement on h, which even does not need to be continuous. We note U_m the largest value for which $h = 0$, and we note U_Y the smallest value for which $h = 1$. They do not necessarily correspond to any singularity in h.

2. Examples and robustness

Table I proposes a few examples of yield functions h.

We can interpolate between abrupt and smooth transitions, using the family of model power-law yield functions:

$$h(U) = \left(\frac{|U|}{U_Y}\right)^n. \tag{6}$$

Yield function h	Elastic response $U(\varepsilon)/U_Y$
$(\lvert U\rvert/U_Y)^0$	0
$(\lvert U\rvert/U_Y)^1$	$1-\exp(-\varepsilon/U_Y)$
$(\lvert U\rvert/U_Y)^2$	$\tanh(\varepsilon/U_Y)$
$\sin^2(\lvert U\rvert/U_Y)$	$\arctan(\varepsilon/U_Y)$
$(\lvert U\rvert/U_Y)^\infty \approx \mathcal{H}(\lvert U\rvert/U_Y-1)$	$\varepsilon-\mathcal{H}(\varepsilon/U_Y-1)\varepsilon$

TABLE I: Elastic deformation for several yield function h, for a non-deformed initial condition $U(0)=0$ and with $\dot\varepsilon$ of constant sign.

With these functions plasticity appears more or less gradually, as soon as $|U|>0$. That is, $U_m=0$. The limit $n\to\infty$ is the discontinuous Heaviside function:

$$h(U)=\mathcal{H}(|U|-U_Y). \tag{7}$$

An example of a yield function with finite U_m is a piece-wise linear function, $h=0$ for $|U|\le U_m$ and $h=(|U|-U_m)/(U_Y-U_m)$ for $|U|\ge U_m$.

More generally, the yield function can be thought as the convolution of the Heaviside function $\mathcal{H}$ and a distribution of yield values p_Y:

$$h(U)=p_Y(U_Y)\otimes\mathcal{H}(|U|-U_Y). \tag{8}$$

We can now interpret the discontinuous yield function (7) as the result of a distribution of yield values which is a Dirac function centered on U_Y. Note that (8) is equivalent to an integration (indeed a Dirac distribution of yield values provides a Heaviside yield function).

D. Contributions to total stress

We consider two separate contribution to stress.

The elastic stress is proportionnal to the elastic strain U (see test in [14]):

$$\sigma^{\rm el}=\mu U, \tag{9}$$

where μ is the shear elastic modulus.

The viscous contribution to the stress is due to large scale velocity gradients: $\sigma^{\rm vis}=\eta\dot\varepsilon$ (see model proposed by [7, 22]). Here η is a macroscopic viscosity.

We assume, for simplicity and in the same spirit as in a polymeric model [4], that the stresses add up:

$$\begin{aligned}\sigma &= \sigma^{\rm el}+\sigma^{\rm vis}\\ &= \mu U+\eta\dot\varepsilon.\end{aligned} \tag{10}$$

At high applied shear, the elastic stress $\sigma^{\rm el}$ saturates at a value close to the yield stress $\sigma_Y=\mu U_Y$, where μ is the shear modulus and U_Y is the yield strain.

To maintain a steady shear rate thus requires a stress which has two components. The first one $\sigma^{\rm el}$, when averaged over a time much larger than $\tau_{\rm relax}$, appears as a plateau: that is, a constant stress σ_Y. The dissipative power is proportional to $\dot\varepsilon$. It is thus typical of a Coulomb friction model [23, 24], that is a solid (plastic) behaviour, although its physical origin lies in microscopic viscous dissipation. The second one is a classical fluid behaviour: its contribution to stress is $\eta\dot\varepsilon$; the corresponding dissipated power is quadratic, proportionnal to $\dot\varepsilon^2$.

III. PREDICTION AND TESTS

A. Transient response from rest

Here, we calculate the transient response during a shearing experiment, that is, the relation $U(\varepsilon)$ between applied strain ε and elastic strain U. For simplicity we take here $\varepsilon=U=0$ at the start of the experiment, but that assumption is easy to relax.

By direct integration, eq. (5) yields:

$$\varepsilon=\int_0^U\frac{{\rm d}U}{1-h(U)}. \tag{11}$$

Calculating this integral yields $\varepsilon(U)$, which can be inverted to obtain $U(\varepsilon)$. These functions are measurable on experiments and can be compared with predictions derived from direct measurements of $h(U)$.

Whatever the function $h(U)$, eq. (11) implies that $U\approx\varepsilon$ near the origin: applied and elastic deformation are almost equal in the elastic regime. At the onset of plasticity (or topological changes), they differ. In fact, the r.h.s. of eq. (11) diverges at $U=U_Y$. Thus, when ε increases arbitrarily, U tends asymptotically towards the saturation value U_Y.

Some functions $U(\varepsilon)$ are given on table I. Since they are very similar, for clarity only some of them are plotted on figure 1. Strikingly, they do not depend much on the actual expression of $h(U)$. In fact, only the expression of h near U_Y matters; the relation between ε and U is robust. The elastic deformation U is close to the imposed strain ε at low applied strain, and tends to a saturation value at large applied strain.

Thus the distribution of bubble sizes does not affect much the foam's transient response (as opposed to the liquid fraction, which drastically affects U_Y [21]). This explains why in the literature the function $U(\varepsilon)$ is sometimes taken for simplicity as a piecewise linear function or as a hyperbolic tangent [25]. For instance, the harmonic expression $h(U)=(U/U_Y)^2$ yields $U(\varepsilon)=U_Y\tanh(\varepsilon/U_Y)$. This provides both the physical origin for the function $\sigma(\varepsilon)$ of the model by Janiaud *et al.* [25], and a justification for their (up to now arbitrary) expression $\sigma=\sigma_Y\ f(\varepsilon/\varepsilon_Y)$: the function f corresponds to the present elastic deformation U, while ε_Y is the yield strain they chose equal to 1 for simplification.

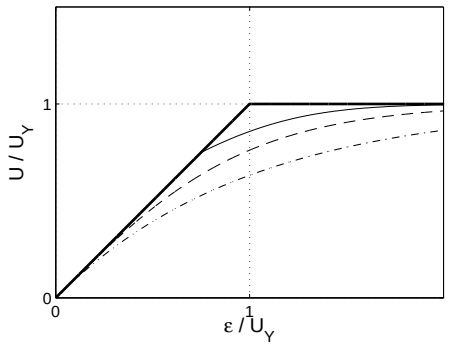

FIG. 1: Response from rest with yield function $h(U) = \mathcal{H}(|U| - U_Y)$ (thick line), $h(U) = (|U| - U_m)/(U_Y - U_m)\mathcal{H}(|U| - U_m)$ with $U_m = 0.75\ U_Y$ (thin line), $h = (U/U_Y)^2$ (dashed line) and $h = (U/U_Y)$ (dash-dotted line).

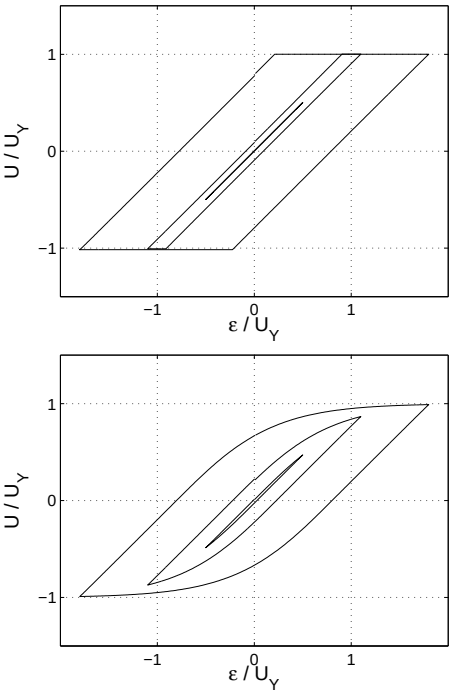

FIG. 2: Periodic response to an oscillatory shear, for three amplitudes: $\varepsilon/U_Y = 0.5, 1.1$ and 1.8. Top: Plasticity appears abruptly at the critical value U_Y. Bottom: Plasticity appears smoothly, $h = (U/U_Y)^2$.

B. Hysteresis cycle

A typical rheometry experiment, for instance in a Couette apparatus [9, 11, 17, 26], measures the stress $\sigma(t)$ on the walls while imposing an applied sinusoidal shear strain of pulsation $\omega = 2\pi/T$:

$$\varepsilon = \gamma \sin(\omega t). \tag{12}$$

To test the hysteresis of the model we calculate the response to such a periodic oscillatory shear bounded by amplitudes γ and $-\gamma$.

The periodic elastic deformation *vs* strain curve is plotted figure 2 top (after numerical integration of equations 4 and 7). The stress response is linear in strain below the threshold, and saturates above in plastic regime, exhibiting a strong hysteresis.

A smooth transition from elastic to plastic, using $h = (U/U_Y)^2$, provides smooth variation of deformation as a response of load: see the results of a numerical integration of figure 2 bottom.

Reversing the sign of the loading instantly stops any plasticity and the reponse becomes purely elastic. Multiple loadings do not increase the slope of the loading part, nor the value of saturation yield. Such features are observed in experiments on other amorphous solids [27, 28] (as opposed to strain-hardening features of crystalline metals [2]).

C. Storage and loss moduli

1. *Predictions for a non-linear response*

In complex notation the stress response σ^* is linked to the strain ε^* by $\sigma^* = (G' + iG'')\varepsilon^*$, with G' the storage modulus and G'' the loss modulus of the material, defined as the in-phase and out phase part of the response (first term in a Fourier series, see non linear models [29–31]).

When increasing the amplitude γ of the imposed sinusoidal shear strain, the response is first linear until the amplitude at which G' and G'' start to vary. In both the linear and non-linear regimes, the storage and loss moduli are calculated as:

$$\begin{aligned} G' &= -\frac{1}{\gamma^2}\frac{1}{\pi\omega}\int_0^T \sigma(t)d\dot{\varepsilon}, \\ G'' &= \frac{1}{\gamma^2}\frac{1}{\pi}\int_0^T \sigma(t)d\varepsilon, \end{aligned} \tag{13}$$

G' is proportionnal to the area enclosed by the $(\sigma(t), \dot{\varepsilon}(t))$ curve, while G'' is proportional to the area enclosed by the $(\sigma(t), \varepsilon(t))$ curve. When plasticity occurs, the cycle has a non-vanishing area in the $(\sigma(t), \varepsilon(t))$ diagram, meaning a non-vanishing loss modulus G''.

In the present model $\sigma(t)$ depends on the current elastic strain $U(t)$ and shear rate $\dot{\varepsilon}(t)$ (eq. 10). For the case of the abrupt elastic/plastic transition $h = \mathcal{H}(|U| - U_Y)$, the analytical integration of areas is simple and provides the following solutions for the moduli. Using eqs. (13) we obtain, when $\gamma \ll U_Y$:

$$\begin{aligned} G' &\simeq \mu \\ G'' &= \eta, \end{aligned} \tag{14}$$

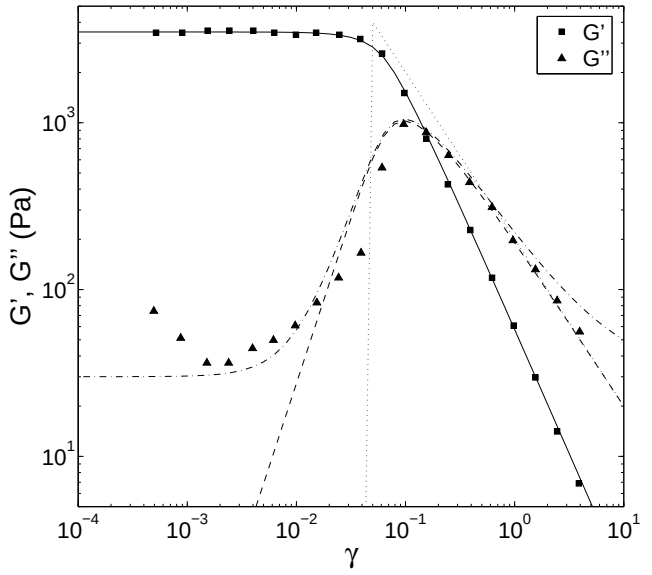

FIG. 3: Emulsion storage and loss moduli *versus* strain amplitude. Symbols: experimental G' (circles) and G'' (triangles) in a close-packed emulsion, fraction of the continuous phase 20%, droplet size 0.53 μm, oscillation pulsation $\omega = 1$ rad s^{-1} (Fig. 1 of ref. [32]). Material specific parameters: shear modulus $\mu = 1.7\ 10^3$ Pa, yield strain $U_Y = 0.045$, viscosity $\eta = 30$ Pa.s. Lines : quasistatic models of G' (solid line), and of G'' with an abrupt yield function $h = \mathcal{H}(|U| - U_Y)$ (dotted line), with a smooth yield function $h = (U/U_Y)^2$ (dashed line), and the same smooth h with viscosity (dash-dotted line).

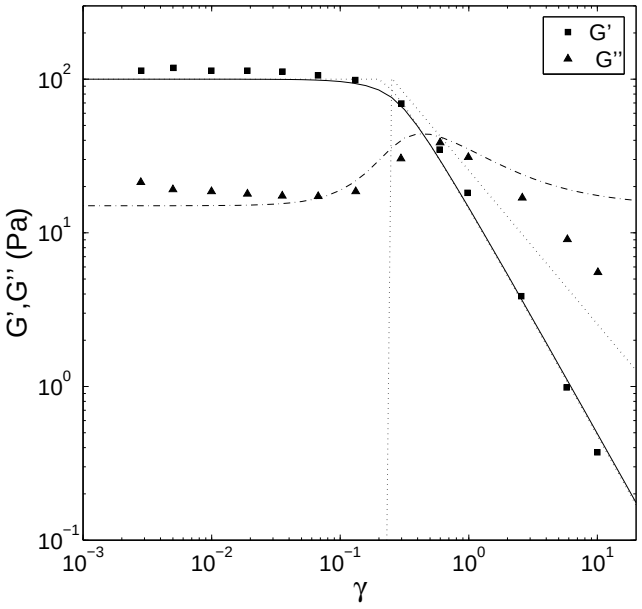

FIG. 4: Same as Fig. (3) for a polydisperse foam [33]. Liquid fraction 5%, bubble size 40 to 70 μm, $\omega = 1$ rad s^{-1}. Material specific parameters: $\mu = 100$ Pa, $U_Y = 0.2$, viscosity $\eta = 15$ Pa.s.

and when $\gamma \gg U_Y$:

$$G' \simeq \mu \frac{4}{\pi} \left(\frac{U_Y}{\gamma} \right)^{3/2},$$
$$G'' = \mu \frac{4U_Y}{\pi\gamma} + \eta. \qquad (15)$$

For smooth yield function h, we perform a numerical integration. The corresponding predictions are plotted on Figs. (3-5).

2. *Comparison with experiments on emulsions and foams*

Rheometry measurements of monodisperse emulsion [32] (Fig. 3) and polydisperse foams [26, 33] (Figs. 4,5). directly yield, without hypotheses, the values of the material parameters required by the model. The shear modulus μ is read from the value of G' at low amplitude. The viscosity η is read from the value of G'' at low amplitude (or the value of the minimum, in Fig. 3). The yield strain U_Y is read from the intersection of low amplitude plateau of G' and its large amplitude $-3/2$ exponent power-law.

A purely elasto-plastic model is enough to predict G' correctly, over the whole range of amplitude, including the $-3/2$ exponent power-law. R. Höhler (private communication) obtained similar analytical results to model

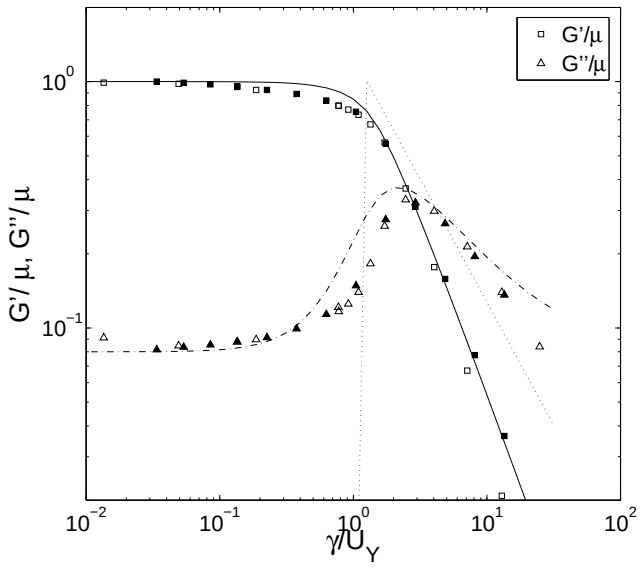

FIG. 5: Same as Fig. (3) for a monodisperse foam [26]. Liquid fraction 8%, bubble size 21 μm, $\omega = 1$ rad s^{-1}. Data of G' and G'' are normalised by μ and γ by U_Y, while $\eta\omega/\mu = 0.08$.

data of Fig. 5. This simplest model also describes correctly the large amplitude trend for G''.

The low amplitude value of G'' can be modelled by including a viscosity (which confirms that viscosity is relevent even in such quasistatic models), at the expense of a slight overprediction at large amplitudes. This latter aspect suggests a possible shear-thinning, that is a decrease of the viscosity η with the shear rate, similarly

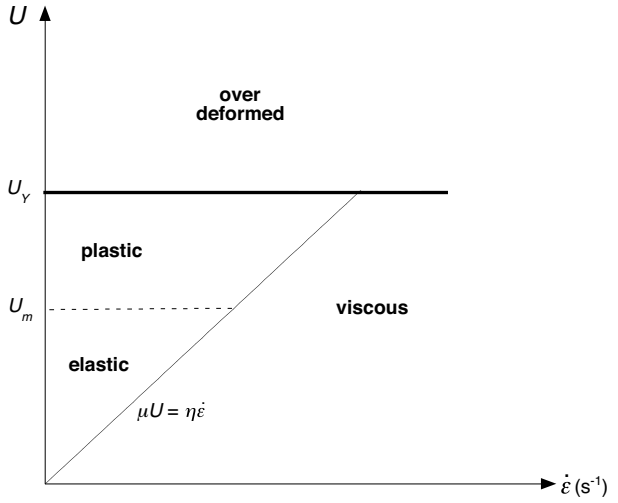

FIG. 6: Scalar quasistatic phase diagram for a foam or an emulsion. Axes are experimentally measurable [20] local variables: shear rate $\dot{\varepsilon}$ and elastic strain U. The crossover from elastic to plastic is defined as the onset of the first isolated topological rearrangements. The crossover from solid to fluid is defined by the equality of viscous and elastic stresses. The yield strain U_Y corresponds to a macroscopic rate of topological rearrangements. The quasistatic regime presented here ceases to be valid when $\dot{\varepsilon}$ becomes comparable to $\tau_{\rm relax}^{-1}$, inverse of the microscopical relaxation time.

to the observed reduction of the drag of foams in motion in channels [21].

The agreement between the data and the model, without adjustable parameter, becomes remarquable even for G'' at intermediate amplitudes, if we use a smooth yield function h, such as $h = (U/U_Y)^2$ (dash-dotted lines). If we had a direct experimental measurement of h, we could inject it in the model to predict G'' at intermediate amplitudes, near U_Y, but the resulting predictions would probably be very similar. In fact, the curves are robust with respect to h; this implies that, conversely, we are not yet able to deduce h from G'' data.

Note that this scalar approach does not take into account the influence of the orientation of material deformation inside the Couette apparatus. The measured Couette variables are actually tensorial components, $\sigma_{12} = \sigma$ (tangential force per unit wall surface) and $\varepsilon_{12} = \varepsilon/2$ (components of the symmetrized deformation gradient), in a coordinate system aligned with walls. Preliminary work [34] shows that, at low amplitudes, the scalar model predictions coincides with tensorial predictions for shear and loss modulus in a Couette rheometer.

IV. REPRESENTATIONS

A. Phase diagram

In a given experiment, the current state of a region of the foam (representative volume element, or RVE) is characterised by two local quantities: the local elastic strain U, and the local shear rate $\dot{\varepsilon}$. Both of course depends on the sample's past history, but this history plays no explicit role. Both are always defined, whether in elastic, plastic or viscous regime [13]. Each volume element can thus be plotted as a point in a phase diagram (Fig. 6); that is, the $(\dot{\varepsilon}, U)$ plane. In a heterogeneous flow, different volume elements of the same foam are plotted as different points. A volume element's evolution is a trajectory on this plane.

The crossover between elastic and plastic regime occurs around U_Y, with possible precursors around U_m. The crossover from both regimes to the viscous one occurs when the viscous contribution to the stress becomes larger than the elastic one. Fig. (6) thus plots the line:

$$\mu U = \eta\dot{\varepsilon}. \tag{16}$$

This is equivalent to:

$$\mathrm{Wi}_M = U, \tag{17}$$

where we have introduced the macroscopic local Weissenberg number defined as:

$$\mathrm{Wi}_M \equiv \frac{\eta\dot{\varepsilon}}{\mu}. \tag{18}$$

Pure regimes correspond to the axes of the plane: pure elastic and pure plastic on the vertical axis, pure viscous on the horizontal axis.

A deformation beyond U_Y is not accessible when starting from rest (Fig. 6). But of course the foam could initially be prepared (for instance artificially [35]) in a configuration very far from equilibrium. Under a steady shear rate $\dot{\varepsilon}$, the deformation U always tends towards $U_Y(\dot{\varepsilon})$, whether from below or from above.

B. Mechanical analog

The model can be summarized with a mechanical representation (Fig. 7). In a steady state regime, at constant $\dot{\varepsilon}$, $U = U_Y$ and the elastic stress equals the constant yield stress (solid friction like): $\sigma_Y = \mu U_Y$. The total stress is $\sigma = \mu U + \eta\dot{\varepsilon} = \sigma_Y + \eta\dot{\varepsilon}$.

The material is characterised by the coefficients η, μ and U_Y. Measuring experimentally, and understanding theoretically the physical origin of these coefficients, requires specific studies for each material considered: this is beyond the scope of the present paper. In principle, they can be rank-four tensors (anisotropic material). They can even vary with the material's state (non-linear material), for instance in the shear-thinning case mentioned above.

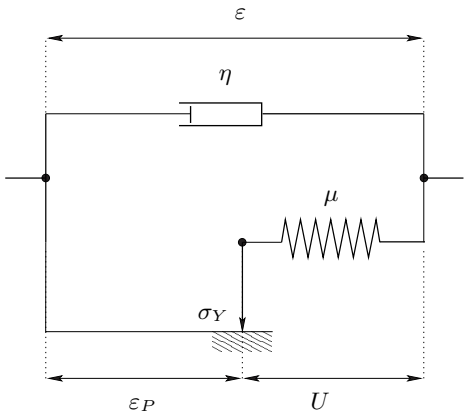

FIG. 7: A linear elasto-visco-plastic rheological model.

C. Visual analogy

A visual analogy is the motion of a brush on a wall (see figure 8). The handle of the brush moves with an oscillatory position ε parallel to the wall (analog of the imposed scalar deformation of the material), while the displacement of the handle with respect to the brush tip is U (the analog of the internal elasticity of the material). The sliding velocity of the contact point is therefore $\dot{\varepsilon}_P$ according to equation 1 and is the analog of plasticity in a material.

The material properties described by the model now apply to the brush bending elastic modulus μ, and the deformation U_Y at onset of sliding. The dissipations are associated with motion of the handle in air with viscous coefficient η.

This analogy visualises the direction and the amplitude of the deformation U, made visible by the brush. This is helpful to obtain intuition on the transient elastic response. The analogy extends to the equations of motion, which are the same as in the previous section, although the physical variables are here completely different (and even have different units).

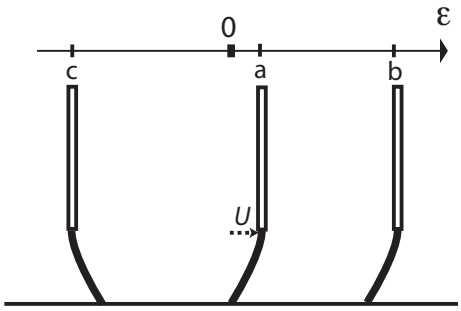

FIG. 8: Analog system: an elastic brush stick/slipping on wall with a viscous slip and a damped handle motion. We represent several states, for an imposed oscillatory "painting-like" motion of the handle, from rest position 0: (a) onset of sliding to the right, (b) far-right position, (c) far-left position.

Acknowledgments

We thank S. Ataei Talebi, I. Cheddadi, B. Dollet, E. Janiaud, C. Quilliet, C. Raufaste, and P. Saramito for discussions, R. Höhler for comparison with his calculations before publication, and F. Rouyer for providing experimental data.

[1] L. D. Landau and E. M. Lifchitz, *Theory of elasticity* (Reed, 1986).
[2] J. Chakrabarty, *Theory of plasticity* (McGraw-Hill Book Company, New York, 1978).
[3] G. K. Batchelor, *An introduction to fluid dynamics* (Cambridge University Press, Cambridge, 2000).
[4] C. W. Macosko, *Rheology : principles, measurements and applications* (Wiley-VCH, 1994).
[5] D. François, A. Pineau, and A. Zaoui, *Comportement mécanique des matériaux: viscosité, endommagement, mécanique de la rupture, mécanique du contact* (Hermès, 1993).
[6] D. François, A. Pineau, and A. Zaoui, *Comportement mécanique des matériaux : élasticité et plasticité* (Hermès, 1995).
[7] A. M. Kraynik, Ann. Rev. Fluid Mech. **20**, 325 (1988).
[8] D. Weaire and S. Hutzler, *The physics of foams* (Oxford University Press, Oxford, 1999).
[9] R. Höhler and S. Cohen-Addad, J. Phys. Cond. Matt. **17**, R1041 (2005).
[10] R. G. Larson, *The structure and rheology of complex fluids* (Oxford University Press, 1999).
[11] T. G. Mason, J. Bibette, and D. A. Weitz, J. Colloid Interface Sci. **179**, 439 (1996).
[12] G. Porte, J.-F. Berret, and J. Harden, J. Phys. II France **7**, 459 (1997).
[13] M. Aubouy, Y. Jiang, J. A. Glazier, and F. Graner, Granular Matt. **5**, 67 (2003).
[14] M. Asipauskas, M. Aubouy, J. A. Glazier, F. Graner, and Y. Jiang, Granular Matt. **5**, 71 (2003).
[15] N. Cristescu and I. Siliciu, *Viscoplasticity* (Martinus Nijhoff, 1982).
[16] A. K. Miller, *Unified constitutive equations for creep and plasticity* (Elsevier Applied Science, 1987).
[17] J. Lauridsen, M. Twardos, and M. Dennin, Phys. Rev. Lett. **89**, 098303 (2002).
[18] A. D. Gopal and D. J. Durian, Phys. Rev. Lett. **91**, 188303 (2003).
[19] A. Kabla and G. Debrégeas, Phys. Rev. Lett. **90**, 258303 (2003).
[20] P. Marmottant, B. Dollet, C. Raufaste, and F. Graner, cond-mat/0609188.
[21] H. M. Princen, J. Coll. Interf. Sci. **91**, 160 (1983).
[22] A. M. Kraynik and M. G. Hansen, J. Rheol. **31**, 175 (1987).
[23] C. A. Coulomb, Mémoires de l'Académie des Sciences

(Paris) (1779).
[24] T. Baumberger, P. Berthoud, and C. Caroli, Phys. Rev. B **60**, 3928 (1999).
[25] E. Janiaud, D. Weaire, and S. Hutzler, Phys. Rev. Lett. **97**, 038302 (2006).
[26] F. Rouyer, S. Cohen-Addad, and R. Höhler, Coll. and Surf. A **263**, 111 (2005).
[27] M. Aubertin, M. R. Julien, S. Servant, and D. E. Gill, Can. Geotech. J. **36**, 660 (1999).
[28] S. Courty, B. Dollet, K. Kassner, A. Renault, and F. Graner, Eur. Phys. J. E **11**, 5359 (2003).
[29] K. Hyun, S. H. Kim, K. H. Ahn, and S. J. Lee, J. Non-Newtonian Fluid Mech. **107**, 51 (2002).
[30] H. G. Sim, K. H. Ahn, and S. J. Lee, J. Non-Newtonian Fluid Mech. **112**, 237 (2003).
[31] K. Miyazaki, H. M. Wyss, D. A. Weitz, and D. R. Reichman, Europhys. Lett. **75**, 915 (2006).
[32] T. G. Mason, J. Bibette, and D. A. Weitz, Phys. Rev. Lett. **75**, 10 (1995).
[33] A. Saint-Jalmes and D. Durian, J. Rheol. **43**, 6 (1999).
[34] C. Raufaste and al., in preparation.
[35] F. Elias, C. Flament, J. A. Glazier, F. Graner, and Y. Jiang, Phil. Mag. B **79**, 729 (1999).